Propagation of Nighttime Medium-Scale Traveling Ionospheric Disturbances (MSTIDs) During High and Low Solar-Activity Conditions

Alexandre Alvares Pimenta

Abstract – Using all-sky imaging systems and a Digisonde 256, measurements of moving medium-scale traveling ionospheric disturbances (MSTIDs) in the OI 630.0 nm nightglow emission were detected in the low latitudes/tropical region. Estimates of the spatial damping decrements for MSTIDs by the theory of magnetohydrodynamics show that the increase in electron concentration in the F region is the main parameter for MSTIDs absorption. From this point of view, we can understand the fact that most moving disturbances covering distances of several thousands of kilometers during low solar activity are recorded probably at heights below the peak of the F layer. In this paper, we present and discuss for the first time the effect of ionization in the absorption of MSTIDs during low and high solar-activity periods.

1. Introduction

Although medium-scale traveling ionospheric disturbances (MSTIDs) were discovered about 70 years ago, they continue to be an important subject of intensive experimental and theoretical investigation because they have an influence on transionospheric radio-wave communications. The main observational techniques used have been ionosondes [1–2], scintillations [3], wide-angle imaging systems [4–6], and global positioning systems [7–8].

Observations of the OI 630 nm nightglow emission using a wide-angle imaging system have been carried out at Cachoeira Paulista, Brazil (22.7°S, 45.0°W, 15.8° dip), during the period from 1989 to 2001. The all-sky images in the OI 630 nm emission obtained during the period from January 1989 to December 1990 and January 2000 to December 2001 (high solar activity [HSA]; average 10.7 cm solar cycle flux $> 160 \times 10^{-22}$ W m^{-2} Hz^{-1}), and January 1995 to December 1996 (low solar activity [LSA]; average 10.7 cm solar cycle flux $< 90 \times 10^{-22}$ W m^{-2} Hz^{-1}) were used to analyze MSTIDs propagation. Our observations of the MSTIDs are not related to disturbed geomagnetic conditions. These structures are aligned from northeast to southwest and drift toward the northwest at an altitude of approximately 220 km to 300 km. Perkins instability might be involved in the generation of these structures in high or midlatitudes that are observed also in the tropical region [9–11].

On the other hand, since the ionospheric F region is a weakly ionized gas, it is assumed that the propagation of the wave in this region is supported solely by the neutral component of the atmosphere, with the ionized portion of the atmosphere set into motion by ion-neutral collisions. Thus, the effects on MSTIDs of the ionization in the F region via ion-neutral collisions can be discussed in terms of magnetohydrodynamic absorption theory. Also, this experimental study presented an opportunity to discover important information on the origin and manner of MSTIDs in the thermosphere/ionosphere region and to investigate the impact on nightglow emission chemistry and dynamics.

Section 2 presents observational measurements and a statistical study of MSTIDs occurrence as a function of solar cycle. Section 3 uses magnetohydrodynamic theory to calculate the absorption of MSTIDs for both low and high solar-activity periods. The paper ends with concluding remarks in Section 4. Particular attention is paid to the effects of electron density in the F region on propagation of MSTIDs during both high and low solar-activity periods.

2. Measurement Technique and Observations

Figure 1 shows the field of view of the all-sky imager together with other relevant information. The OI 630 nm emission is produced in the bottom side of the F region by the dissociative recombination $O_2^+ + e \rightarrow O + O^*(^1D)$, with spontaneous photon emission by the excited oxygen atoms $O^*(^1D) \rightarrow O + h\nu$ (630 nm), and is widely used to monitor important ionospheric processes at F region heights. An important characteristic of the imager is the relationship between zenith angle and image size. A zenith angle of approximately 90° encompasses ±15° latitude/longitude from the zenith, which is equivalent to a horizontal diameter of approximately 3600 km at 275 km altitude [12]. The imaging system uses a 10 cm diameter interference filter with a bandwidth of 1.35 nm and records intensified monochromatic images on 35 mm film using a conventional single-lens reflex camera. The images were recorded at intervals of 20 min with 32 s exposure time. The OI 630 nm image observations were carried out on 12 or 13 nights around new-moon periods, when weather conditions permitted. During the period of nearly 11 years (January 1989 to December 1991 and January 1994 to December 2001) of observations, about

Manuscript received 13 July 2020.

Alexandre Alvares Pimenta is with the National Institute for Space Research–INPE, Avenida Dos Astronautas, 1758, São José dos Campos, SP, Brazil, CEP 12227-010; e-mail: alexandre.pimenta@inpe.br.

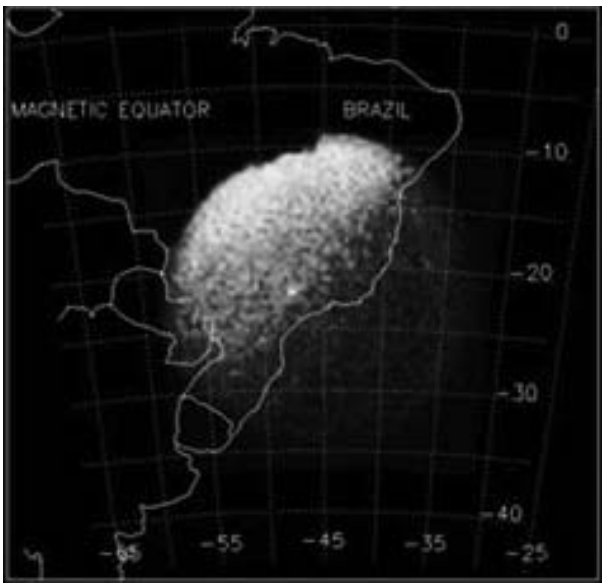

Figure 1. OI 630.0 nm emission all-sky image obtained at Cachoeira Paulista, Brazil, on June 10–11, 1996 at 2400 local time, with its respective field of view (considering an emission height around 275 km).

12,732 good images of OI 630 nm nightglow emission were obtained. More details on the all-sky imager used in this paper can be found in [13].

Figure 2 shows a sequence of images of the OI 630 nm emission obtained on June 10–11, 1996, from 2340 local time to 2440 local time. In this example, the

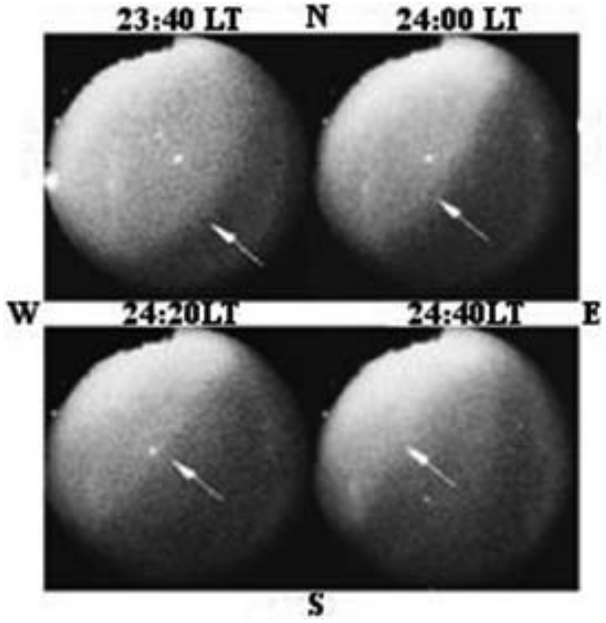

Figure 2. Example all-sky images in the OI 630 nm emission obtained on June 10–11, 1996, from 2340 local time to 2440 local time. The white arrows indicate the MSTIDs (dark structures). The MSTIDs entered from the southeast and moved northwest across the field of view.

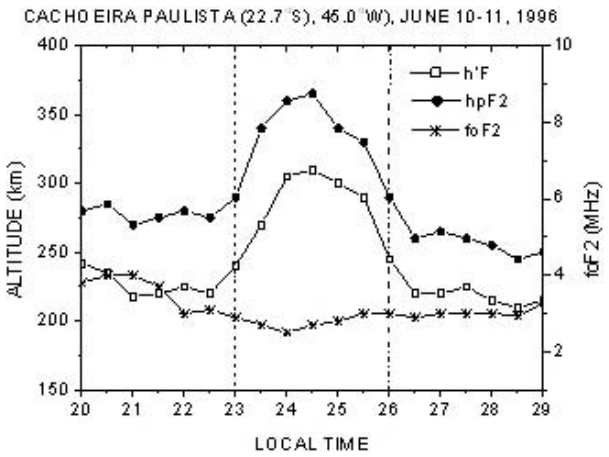

Figure 3. Example of temporal variation of ionospheric parameters hpF2, h′F, and foF2 for the night of June 10–11, 1996. The vertical dashed lines emphasize the abrupt rise of the F layer around 2400 local time during the passage of MSTIDs on the zenith of Cachoeira Paulista.

MSTIDs entered from the southeast and moved northwest across the field of view, with an average speed of about 180 m/s, a horizontal wavelength of 900 km, and a period of 3.0 h to 3.5 h. In order to calculate these parameters, the images were transformed using the unwarping method described by [14–15]. As a complementary tool, a Digisonde 256 (DGS256) located at the same site as the all-sky imager was used to obtain vertical sounding data of the ionosphere. On June 10–11, 1996 (Figure 3), around 24 local time, the Digisonde registered abrupt increases in both F layer peak height (hpF2) and base height (h′F) when the low-intensity band (MSTIDs) passed over Cachoeira Paulista (coinciding with the all-sky image observations). This behavior of the ionospheric parameters is a typical signature of the MSTIDs phenomenon in the midlatitudes [16].

A statistical study of MSTIDs occurrence as a function of solar cycle is shown in Figure 4. The occurrence frequency is exhibited as a percentage of the hours of observation from 1989 to 2001 (two periods of HSA). Gray bars indicate the airglow observations in the OI 630 nm emission, and black the MSTIDs occurrence rate (%). The occurrence frequency is inversely correlated with the solar cycle. Nevertheless, no MSTIDs occurrence is observed during the peaks of HSA (1990 and 2000), and the greatest occurrence is during the period of LSA (1995 and 1996).

3. Discussion

One question that needs to be answered is: Why during high solar-activity periods is the occurrence of MSTIDs extremely low? This section, using the theory of magnetohydrodynamic absorption and ground-based optical and radio-technique observations, shows for the first time that in both low latitudes and tropical regions, the appearance or not of these structures is associated

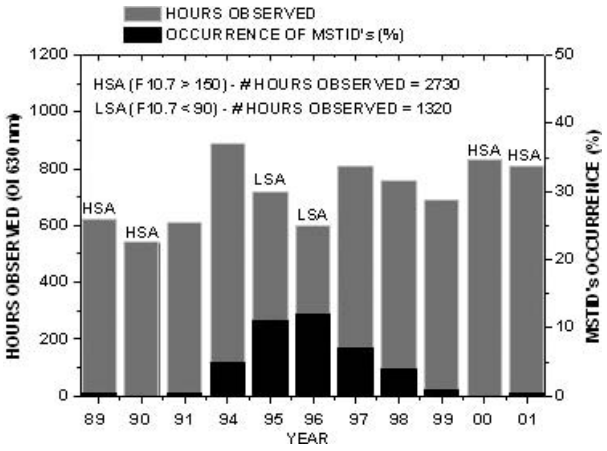

Figure 4. Occurrence of MSTIDs in the low-latitude region during the solar cycle phases. HSA refers to high solar activity (F10.7 > 150), and LSA to low solar activity (F10.7 < 90). Gray bars indicate the airglow observations in the emission OI 630 nm, and black bars the MSTIDs occurrence rate (%).

mainly with the decrease or increase of electron concentration in the F region. So solar-activity periods play an important role in the propagation or absorption of MSTIDs.

A. Absorption of MSTIDs

A good parameter to explain the magnetohydrodynamic absorption of these moving disturbances in the F region, which are generated in high or midlatitudes, is the magnitude of the index of absorption. According to [17], this index can be written as

$$R_x = G\left[1 + \frac{k_x^2}{k_z^2} - \left(\cos\alpha - \frac{\cos\gamma}{k_z}\right)^2\right] \qquad (1)$$

where $G = N_e M \nu_{im} k_x / N_m M_m \omega$; and $\cos\alpha$, $\cos\beta$, and $\cos\gamma$ are the projections on the x-, y-, and z-axes, respectively, of the magnetic-field direction in a Cartesian coordinate system (x is positive to northward, y to eastward, and z to upward); N_e is the electron density (available from Digisonde data); M is the ion mass; ν_{im} is the ion-molecule collision frequency; ω is the wave angular frequency; k_x and k_z are the horizontal and vertical wavenumbers; M_m is the molecular mass; and N_m is the molecule concentration. We can estimate in (1) the value of G independent of the orientation of the magnetic field **B**.

Table 1. Distances D at which wave amplitude decreases by a factor of e during LSA

Altitude (km)	G (cm^{-1})	$D = 1/G$ (km)
220	2.5×10^{-9}	4000
250	6.9×10^{-9}	1500
300	1.6×10^{-8}	625

Table 2. Distances D at which wave amplitude decreases by a factor of e during HSA

Altitude (km)	G (cm^{-1})	$D = 1/G$ (km)
220	1.7×10^{-8}	588
250	4.0×10^{-8}	250
300	1.0×10^{-7}	100

Tables 1 and 2 give values of G (in cm^{-1}) for altitudes of 220 km, 250 km, and 300 km during both low and high solar-activity periods. In these estimates, we use the phase velocity in the horizontal direction $V_{ph} = \omega/k_x = 250$ m/s, obtained from the observations (available from the all-sky imager), and the collision frequencies ν_{im} for the specified altitudes during low and high solar-activity periods. In addition, the molecular concentration is obtained from the MSIS-E-90 model. The expression in square brackets in (1) depends on the orientation of the direction of propagation relative to the field **B**. We can compare the R_x values for propagation of MSTIDs along the meridian, defined in (2) as $(R_x)_m$, and in the east–west direction, defined in (3) as $(R_x)_n$. If we assume that the direction of propagation in the horizontal plane is parallel to the x-axis, the direction of the magnetic meridian coincides approximately with the x-axis and $\cos\beta = 0$. Then from (1) we have

$$(R_x)_m = G\left(\sin\alpha + \frac{k_x\cos\alpha}{k_z}\right)^2 \qquad (2)$$

and for propagation in the east—west direction, $\cos\alpha = 0$ and we obtain

$$(R_x)_n = G\left(1 + \frac{k_x^2\sin^2\gamma}{k_z^2}\right) \qquad (3)$$

In [18] it was shown that under the condition $\omega^2/k_x^2 C_0^2 \ll 1$ (which means that the rate of movement in the horizontal direction is considerably lower than the velocity of sound), the disturbances have $k_x \ll k_z$. Then for very small α (for example in the tropical region), $(R_x)_m = Gk_x^2/k_z^2$, and for large α (high to midlatitudes), $(R_x)_m = G\sin^2\alpha$. It is evident that $(R_x)_m < (R_x)_n$, and the absorption of the disturbance must be minimal in the north–south direction. It is true that at midlatitudes, $(R_x)_m/(R_x)_n \approx 1$ (for meridional propagation, the angle α coincides with magnetic inclination). But as we approach the tropical region, α decreases and conditions are possible where $(R_x)_m/(R_x)_n \ll 1$. Thus at high and midlatitudes, all the directions of propagation of MSTIDs are approximately equal with respect to magnetohydrodynamic absorption. Consequently, $R_x \approx G$.

Tables 1 and 2 show values of G for both low and high solar-activity periods. Considering that the absorption can be expressed by $\exp(-R_x)$, we can find the distances

$$D \approx \frac{1}{G} \tag{4}$$

at which the wave amplitude decreases by a factor of e.

In Table 1, at a height $h = 220$ km (which can represent the F layer's bottom side), we have $D = 4000$ km, and consequently MSTIDs take around 4 h to completely dissipate (considering the phase velocity $V_{ph} = \omega/k_x = 250$ m/s). This space-time estimation of MSTIDs lifetime seems to be reasonable and agrees with the MSTIDs shown in Figure 2. However, around the F layer peak ($h = 300$ km), we have $D = 625$ km, and MSTIDs take around 40 min to completely dissipate. These absorption estimates indicate that the distance of propagation of MSTIDs during an LSA period does not generally exceed 4000 km. It can be expected that maximum absorption takes place in the vicinity of the F layer maximum. From this point of view, it can be understood that most moving disturbances covering distances of several thousands of kilometers (for example, the event on June 10–11, 1996) are recorded probably at heights below this maximum.

However, during an HSA period, as shown in Table 2, MSTIDs do not propagate over long distances. At a height $h = 220$ km, we have $D = 588$ km, and consequently MSTIDs take around 40 min to completely dissipate. Around the F layer peak ($h = 300$ km), we have $D = 100$ km, and MSTIDs take around 7 min to completely dissipate. The short lifetime of MSTIDs during an HSA period can explain why these structures are hardly seen in the low latitudes and tropical region. In addition, [19] showed that the growth rate determined by Perkins is considerably higher during sunspot minimum conditions than during sunspot maximum conditions for comparable altitudes of the ionospheric F layer, and this is consistent with our results.

4. Conclusions

The observed features of MSTIDs during LSA and HSA periods in the low latitudes and tropical region can be summarized as follows:

1) Estimates of absorption index R_x show that the increase in absorption of MSTIDs is associated mainly with the increase in electron concentration during HSA. The short lifetime of MSTIDs during an HSA period can explain why these structures are hardly seen in the low latitudes and tropical region.
2) It can be expected (from Tables 1 and 2) that maximum absorption of MSTIDs takes place in the vicinity of the F layer maximum. Most moving disturbances covering distances of several thousands of kilometers are probably recorded at heights below the F layer maximum during LSA.
3) The structures reported here are aligned from northeast to southwest and drift toward the northwest at an altitude of approximately 220 km to 300 km and are probably generated in the high or midlatitudes. We conjecture that Perkins instability might be involved in the formation of MSTIDs structures.

5. Acknowledgment

This work was partially supported by grant 2019/22559-6 from the financing agency Fundação de Amparo a Pesquisa do Estado de São Paulo—FAPESP.

6. References

1. J. E. Titheridge, "Theory of Moving Ionospheric Disturbances," *Journal of Geophysical Research*, **78**, 4, February 1973, pp. 656-660.
2. J. E. Titheridge, "The Relative Accuracy of Ionogram Analysis Techniques," *Radio Science*, **10**, 6, June 1975, pp. 589-599.
3. S. Basu and M. C. Kelley, "A Review of Recent Observations of Equatorial Scintillations and Their Relationship to Current Theories of F Region Irregularity Generation," *Radio Science*, **14**, 3, May–June 1979, pp. 471-485.
4. F. J. Garcia, M. C. Kelley, J. J. Makela, and C.-S. Huang, "Airglow Observations of Mesoscale Low-Velocity Traveling Ionospheric Disturbances at Midlatitudes," *Journal of Geophysical Research: Space Physics*, **105**, A8, August 2000, pp. 18407-18415.
5. C. Martinis, J. Baumgardner, J. Wroten, and M. Mendillo, "All-Sky Imaging Observations of Conjugate Medium-Scale Traveling Ionospheric Disturbances in the American Sector," *Journal of Geophysical Research: Space Physics,* **116**, A5, May 2011, A05326.
6. C. Cesaroni, L. Alfonsi, M. Pezzopane, C. Martinis, J. Baumgardner, et al., "The First Use of Coordinated Ionospheric Radio and Optical Observations Over Italy: Convergence of High- and Low-Latitude Storm-Induced Effects," *Journal of Geophysical Research: Space Physics*, **122**, 11, September 2017, pp. 11794-11806.
7. A. Husin, M. Abdullah, and M. A. Momani, "Observation of Medium-Scale Traveling Ionospheric Disturbances Over Peninsular Malaysia Based on IPP Trajectories," *Radio Science*, **46**, 2, April 2011, RS2018.
8. I. Zakharenkova, E. Astafyeva, and I. Cherniak, "GPS and GLONASS Observation of Large-Scale Traveling Ionospheric Disturbances During the 2015 St. Patrick's Day Storm, "*Journal of Geophysical Research: Space Physics*, **121**, 12, November 2016, pp. 12138-12156.
9. M. C. Kelley and C. A. Miller, "Electrodynamics of Midlatitude Spread *F* 3: Electrohydrodynamic Waves? A New Look at the Role of Electric Fields in Thermospheric Wave Dynamics," *Journal of Geophysical Research: Space Physics*, **102**, A6, June 1997, pp. 11539-11547.
10. C. Martinis, J. Baumgardner, J. Wroten, and M. Mendillo, "Seasonal Dependence of MSTIDs Obtained From 630.0 nm Airglow Imaging at Arecibo," *Geophysical Research Letters*, **37**, 11, June 2010, L11103.
11. Q. Zhou, J. D. Mathews, C. A. Miller, and I. Seker, "The Evolution of Nighttime Mid-Latitude Mesoscale F-Region Structures: A Case Study Utilizing Numerical Solution of the Perkins Instability Equations," *Planetary and Space Science*, **54**, 7, July 2006, pp. 710-718.
12. M. Mendillo and J. Baumgardner, "Airglow Characteristics of Equatorial Plasma Depletions," *Journal of*

Geophysical Research: Space Physics, **87**, A9, September 1982, pp. 7641-7652.

13. A. A. Pimenta, P. R. Fagundes, J. A. Bittencourt, and Y. Sahai, "Relevant Aspects of Equatorial Plasma Bubbles Under Different Solar Activity Conditions," *Advances in Space Research*, **27**, 6–7, 2001, pp. 1213-1218.
14. F. J. Garcia, M. J. Taylor, and M. C. Kelley, "Two-Dimensional Spectral Analysis of Mesospheric Airglow Image Data," *Applied Optics*, **36**, 29, 1997, pp. 7374-7385.
15. A. A. Pimenta, P. R. Fagundes, J. A. Bittencourt, Y. Sahai, D. Gobbi, et al., "Ionospheric Plasma Bubble Zonal Drift: A Methodology Using OI 630 nm All-Sky Imaging Systems," *Advances in Space Research*, **27**, 6–7, 2001, pp. 1219-1224.
16. G. G. Bowman, "A Review of Some Recent Work on Midlatitude Spread-*F* Occurrence as Detected by Ionosondes," *Journal of Geomagnetism and Geoelectricity*, **42**, 2, 1990, pp. 109-113.
17. A. A. Pimenta, M. C. Kelley, Y. Sahai, J. A. Bittencourt, and P. R. Fagundes, "Thermospheric Dark Band Structures Observed in All-Sky OI 630 nm Emission Images Over the Brazilian Low-Latitude Sector," *Journal of Geophysical Research: Space Physics*, **113**, A1, January 2008, A01307.
18. J. E. Titheridge, "Large-Scale Irregularities in the Ionosphere," *Journal of Geophysical Research*, **68**, 11, June 1963, pp. 3399-3407.
19. M. C. Kelley and S. Fukao, "Turbulent Upwelling of the Mid-Latitude Ionosphere: 2. Theoretical Framework," *Journal of Geophysical Research: Space Physics*, **96**, A3, March 1991, pp. 3747-3753.